Chinese Journal of Chemical Engineering 85 (2025) 158–166

Contents lists available at ScienceDirect

Chinese Journal of Chemical Engineering

journal homepage: www.elsevier.com/locate/CJChE

Full Length Article

# Lower size limit of raw coal for efficient beneficiation in air-fluidized bed with magnetite particles

Yalong Cao, Donghui Liu, Quanhong Zhu *

*College of Chemical Engineering, Qingdao University of Science and Technology, Qingdao 266042, China*

ARTICLE INFO

*Article history:*
Received 20 February 2025
Received in revised form
23 May 2025
Accepted 27 May 2025
Available online 4 June 2025

*Keywords:*
Raw coal
Dry beneficiation
Fluidized bed
Lower size limit
Magnetite particles

ABSTRACT

A feasible criterion was established to determine the lower size limit of raw coal ($d_{pRm}$) for efficient beneficiation in the air-fluidized bed with magnetite particles. The feasibility of using small magnetite particles to accommodate the fine raw coal was demonstrated from the experimental perspective. The minimum size for the magnetite particles to be fluidized smoothly was clarified as 47.1 μm, which corresponded to the border between Geldart-B and -A groups. Since the gangue and coal components in the raw coal were crushed into the same size, $d_{pRm}$ depended on the greater one between $d_{pGm}$ (minimum size required for the gangue particles to sink towards the bottom) and $d_{pCm}$ (minimum size required for the coal particles to float towards the top). $d_{pGm}$ was determined as 259 μm by supposing that provided the gangue particles accumulated in the lower half bed, they could be potentially extracted from the bottom. On the other hand, it was observed that the coal particles could always accumulate in the upper half bed. Under such circumstances, $d_{pCm}$ was revealed as 9.8 μm since finer coal particles would be blown out by air before the 47.1 μm sized magnetite particles became fluidized. Eventually, $d_{pRm}$ was clarified as 259 μm, agreeing with the common view that raw coal coarser than 6 mm could be effectively beneficiated in the air-fluidized bed with magnetite particles. Additionally, the difficulty in beneficiating the fine raw coal was revealed to arise more from the remixing of sorted gangue particles than that of separated coal particles.


## 1. Introduction

Gangue is generally embedded in the run-of-mine coal. Its removal after the comminution (known as beneficiation/preparation/separation/cleaning) is of paramount significance to alleviating the pollution related to $SO_2$ emission [1] and other problems resulting from the ash formation [2,3]. Such preprocessing of raw coal can also reduce the transportation cost [1,4–7] and raise the calorific value [1,4–6], thus decreasing the carbon footprint throughout the entire lifecycle [8–10]. The separation between the gangue and coal components generally relies on their density difference. The latter usually has a density smaller than 1800 $kg\cdot m^{-3}$ while the density of the former is much greater [4,5,11]. When the raw coal particles are fed into a suitable medium, the heavy gangue particles will deposit at the bottom whereas the light coal particles will float on the top surface.

The wet beneficiation process prevails in the industry. Yet, it suffers severely from the huge consumption of water [12] and relevant environmental pollution. To separate 1 t of raw coal, 3–5 $m^3$ of water is typically required with 0.1–0.2 $m^3$ being lost [2,13]. What's worse, the usage of water is restricted under the following circumstances [14,15]. (1) Water resources are not always available in the arid areas [16–19]. (2) There are problems related to freezing in the cold areas [2,5,15,19,20]. (3) Some young/low-rank coal (*e.g.*, lignite) tends to slime/degrade in water [10,13,19–22]. (4) Subsequent dewatering is necessary before coal transportation and combustion [4,5]. (5) Water pollution is strictly prohibited. The dry beneficiation approach is an attractive alternative to face these situations.

Among the existing dry beneficiation technologies, the air-fluidized bed is efficient and promising [2,20]. The medium particles being bubbling fluidized therein exhibit a pseudo-fluid characteristic and have an apparent bulk density. Such a bubbling fluidized bed is well known as the air-dense medium fluidized bed (ADMFB). When the raw coal particles are fed into the ADMFB, the

* Corresponding author.
*E-mail addresses:* zhuqh87@163.com, zhuqh@qust.edu.cn (Q. Zhu).

https://doi.org/10.1016/j.cjche.2025.05.009
1004-9541/

gangue and coal particles are expected to stratify/segregate according to the deviation of their density from the bed density. Magnetite particles are generally employed as the medium particles due to their abundant reserve, low price, and easy recovery.

Raw coal ranging from 6 to 50 mm has been commercially beneficiated in the conventional ADMFB where the 150–300 μm sized magnetite particles or their mixture with 0.3–1.0 mm sized coal powders served as the dense medium [1,2,7–9,13–15,18,20,23,24]. The so-called probable error was measured to be lower than 0.1. However, the problem of mismatch occurred when the raw coal finer than 6 mm was handled [6,14]. Some coal particles were observed at the lower part of the bed while some gangue particles were detected in the upper part, causing the probable error to exceed 0.1. To conclude, whether a particle would sink or float in the ADMFB depended not merely on its density but also on its size, which was beyond explanation by the Archimedes principle [6].

From our perspective, the unique sinking/floating behavior of particles in the ADMFB results eventually from the rising of gas bubbles and the bubble-induced macro circulation of medium particles (also referred to as gulf streaming [25,26]) [9,11]. For one thing, the rising gas bubbles can lift/carry some of the fine gangue particles which have already deposited on the gas distributor upward and backward into the medium particles [2,8,14]. For another, the descending of medium particles in the near-wall region can entrain some of the fine coal particles that have already floated on the top surface downward and backward into the medium particles. To sum it up, there is remixing (back-mixing only during the continuous separation) of the feedstock particles that have already precipitated from the medium particles [17,27–29]. Nevertheless, it was not further pointed out that either the remixing of the gangue particles or that of the coal particles was more severe. Note that as for the raw coal coarser than 6 mm, the motion of gas bubbles and medium particles is not strong enough to motivate the so-called remixing. In this case, their sinking or floating depends only on the competition between the gravity and buoyancy, irrelevant to the drag force exerted on the particles.

On the other hand, with the rapid development of mechanical mining, more and more fine raw coal is produced and needs beneficiation [1,7,30]. Measures are urgently required to reduce the lower size limit or minimum size of raw coal ($d_{pRm}$) for efficient beneficiation in the air-fluidized bed with magnetite particles. Among others, it was reckoned that $d_{pRm}$ could be reduced simply by deploying smaller magnetite particles [31,32]. Since lower gas velocities were sufficient to fluidize them, the remixing of sorted gangue and/or coal particles could be alleviated to a great extent. Luo and Chen [20] reported that raw coal as small as 6 mm could be handled effectively by the 150–300 μm sized magnetite particles. Choung *et al.* [8] found that raw coal as fine as 1 mm could be effectively treated by the 75–45 μm sized magnetite particles. On the other hand, Sahan and Kozanoglu [4] reported that raw coal as small as 106 μm could be beneficiated efficiently in the traditional ADMFB although the size of magnetite particles was not mentioned. Apparently, there is still a huge controversy about $d_{pRm}$ for efficient beneficiation in the air-fluidized bed with magnetite particles. In fact, no convincing benchmark is available for determining $d_{pRm}$ in the literature. The purpose of this work was to ascertain such a controversy by proposing a feasible criterion. The relevant findings could facilitate the rational design and operation of the conventional ADMFB, thereby maximizing its performance.

## 2. Theoretical

Since there exists no trustful criterion for determining $d_{pRm}$, the following procedures are conceived by us. (1) For the magnetite particles with a given size ($d_{pM}$), the critical size required for the heavy gangue particles ($d_{pGc}$) to sink and that for the light coal particles ($d_{pCc}$) to float are determined. The relationship between $d_{pGc}$ and $d_{pM}$ as well as that between $d_{pCc}$ and $d_{pM}$ are then established. How $d_{pGc}$ and $d_{pCc}$ are determined for a given $d_{pM}$ will be thoroughly introduced in the next paragraph. (2) The smallest magnetite particles with a good fluidization quality can be determined from the classification of particles by Geldart [33]. According to previous research [24], the minimum $d_{pM}$ (denoted as $d_{pMm}$) can be identified as the border between Geldart-B and -A groups (the blue dashed line in Fig. 1). (3) The smallest value for $d_{pGc}$ (specified as $d_{pGm}$) can be deduced from the extrapolation of the $d_{pGc}$–$d_{pM}$ relationship established in step 1 to $d_{pM} = d_{pMm}$. Similarly, the minimum value for $d_{pCc}$ (denoted as $d_{pCm}$) could be acquired *via* extrapolating the as-established $d_{pCc}$–$d_{pM}$ relationship to $d_{pM} = d_{pMm}$. (4) Given that the gangue and coal components in the raw coal are crushed into the same size, the greater one between $d_{pGm}$ and $d_{pCm}$ eventually determines $d_{pRm}$. Based on the above analyzes, the aforementioned controversy about $d_{pRm}$ can be further deemed to stem from that both the $d_{pGc}$–$d_{pM}$ and $d_{pCc}$–$d_{pM}$ relationships are still not well established in the literature.

$d_{pGc}$ and $d_{pCc}$ corresponding to a given $d_{pM}$ can be determined as follows. When the raw coal particles are fed into the air-fluidized bed with magnetite particles, the heavy gangue particles are usually extracted from the bottom whereas the light coal particles are withdrawn from the top surface. Based on this rule, $d_{pGc}$ can be determined from analyzing whether the introduced gangue particles will accumulate in the lower half of the ADMFB. It is assumed in this study that as long as the gangue particles in the lower half bed exceeds 50% of the total in the whole bed, they can be potentially extracted from the bottom. On the other hand, $d_{pCc}$ can be determined from checking whether the introduced coal particles will accumulate in the upper half of the ADMFB. Supposing the coal particles in the upper half bed exceeds 50% of the total in the whole bed, they can be potentially withdrawn from the top surface.

## 3. Experimental

### 3.1. Experimental setup

Two fluidized bed separators (Fig. 2) were employed in this study. Both fluidization columns had an inner diameter of 40 mm and were made of transparent Plexiglass to ease visual observation of segregation. For the fluidization column illustrated in Fig. 2(a), a magnet and a Gaussmeter probe were assigned at the opposite sides [34]. The fluidization column depicted in Fig. 2(b) was specially designed with two sections which were connected by a pair of flanges; the lower section had a height of 40 mm and the

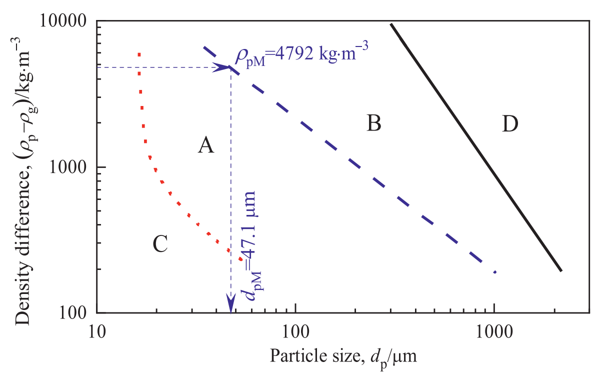


**Fig. 1.** Geldart classification of particles.

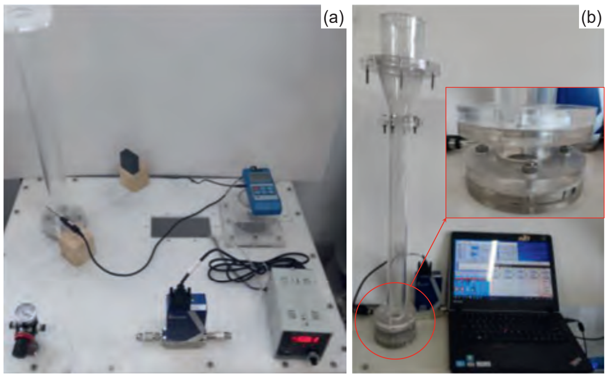


**Fig. 2.** Experimental setup.

upper section 350 mm. An expanded section could be assigned at the top of each fluidization column to alleviate the elutriation of fine particles. The gas distributor was a sintered metal plate with a thickness of 5 mm and an equivalent pore size of 10 μm.

### 3.2. Materials

Air at ambient pressure and temperature served as the fluidizing gas. The desired variation of its flow rate over time could be easily achieved with the aid of a mass flow meter (CS200A, Sevenstar, China). Physical properties of magnetite, gangue, and coal particles (anthracite from Jincheng, Shanxi Province, China) are summarized in Table 1. The Sauter mean diameter ($d_p$) was calculated from the size distribution (Fig. 3) which was usually measured using a laser particle size analyzer (Mastersize 3000, Malvern Panalytical, UK). For the particles coarser than 1500 μm, the size distribution was measured based on the digital image analysis. The particle density ($\rho_p$) was measured *via* the classical drainage method [35–37]. The bulk density ($\rho_b$) was measured from the settled state, which was prepared *via* decreasing gas flow from complete fluidization to zero at a rate of ~0.033 $m\cdot s^{-2}$ [37]. The minimum fluidization velocity ($U_{mf}$) was determined from the bed pressure drop profile ($\Delta P_b$–$U_g\uparrow$) which was recorded during the stepwise increase of gas flow from zero to complete fluidization [38–40]. For the ease of narration, the minimum fluidization velocities for magnetite, gangue, and coal particles were specified as $U_{mfM}$, $U_{mfG}$, and $U_{mfC}$, respectively. Similarly, the average sizes were denoted as $d_{pM}$, $d_{pG}$, and $d_{pC}$; the densities were represented by $\rho_{pM}$, $\rho_{pG}$, and $\rho_{pC}$.

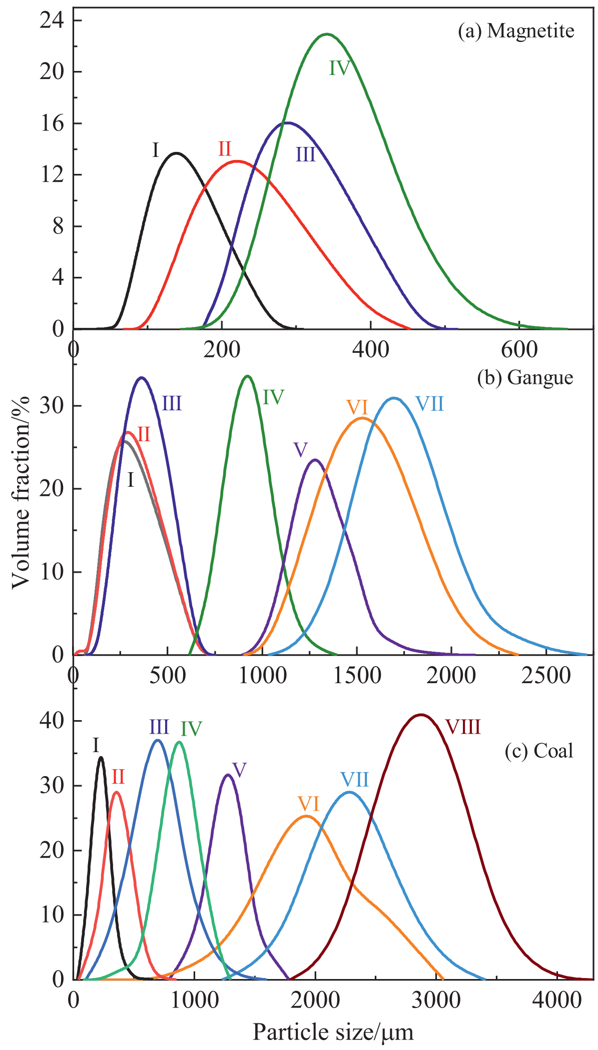


**Fig. 3.** Size distributions of various particles.

**Table 1**
Physical properties of magnetite, gangue, and coal particles.

| Particles | $d_p$/μm | $\rho_p$/kg·m$^{-3}$ | $\rho_b$/kg·m$^{-3}$ | $U_{mf}$/m·s$^{-1}$ |
|---|---|---|---|---|
| Magnetite-I | 139 | 4792 | 2280 | 0.041 |
| Magnetite-II | 213 | | 2260 | 0.129 |
| Magnetite-III | 289 | | 2360 | 0.208 |
| Magnetite-IV | 357 | | 2345 | 0.273 |
| Gangue-I | 207 | 2613 | 1297 | 0.073 |
| Gangue-II | 387 | | 1382 | 0.123 |
| Gangue-III | 661 | | 1409 | 0.227 |
| Gangue-IV | 864 | | 1430 | 0.427 |
| Gangue-V | 1359 | | 1476 | 0.557 |
| Gangue-VI | 1824 | | 1480 | 0.671 |
| Gangue-VII | 2375 | | 1479 | 0.711 |
| Gangue-VIII | 2745 | | 1470 | 0.970 |
| Coal-I | 194 | 1459 | 665 | 0.051 |
| Coal-II | 322 | | 676 | 0.086 |
| Coal-III | 594 | | 690 | 0.194 |
| Coal-IV | 785 | | 717 | 0.407 |
| Coal-V | 1224 | | 749 | 0.463 |
| Coal-VI | 1707 | | 765 | 0.490 |
| Coal-VII | 2173 | | 766 | 0.507 |
| Coal-VIII | 2675 | | 784 | 0.577 |

### 3.3. Operation procedures

#### 3.3.1. Measurement of suspension density

Magnetite particles with known mass were poured into the fluidization column, producing a static height of ~80 mm. During the stepwise decrease of gas flow from $4U_{mfM}$ to $U_{mfM}$, the inventory height ($L$) was recorded on line using a laser rangefinder (GLC30-23, Bosch, China). Finally, the volume occupied by the fluidizing particles was calculated and the suspension density ($\rho_{bM}$) was derived.

#### 3.3.2. Measurement of segregation for magnetite–gangue binary mixture

87.5 ml magnetite and 12.5 ml gangue particles were filled into the fluidization column (Fig. 2(a)) to form a static height of 80 mm. The following two procedures were adopted to acquire the so-called stable fluidization state [41,42]. First, the binary particles were fluidized at $1.5U_{mfG}$ or $4U_{mfM}$ (depending on who was greater) for 5 min to gain good mixing. Then the gas flow was decreased to the target $U_g$ at a rate of $10^{-4}$ m·s$^{-2}$ or less. Then the well-known gas cutting-off method [43,44] was adopted to measure segregation between the binary particles. After the settled state was obtained, $\eta_{G,low}$ (percentage of feeding gangue particles in the lower half bed) could be deduced from the value read from the Gaussmeter [34].

### 3.3.3. Measurement of segregation for magnetite–coal binary mixture

Procedures similar to those summarized in Section 3.3.2 were adopted to measure segregation for the binary mixture of magnetite and coal particles. In particular, the coal particles were poured into the bed after the pouring of magnetite particles. The fluidization column illustrated in Fig. 2(b) was used. After the settled state was obtained, particles in the upper half were taken out by releasing the pair of flanges. These particles were separated using a magnet and weighed to calculate $\eta_{C,up}$ (percentage of feeding coal particles in the upper half bed).

## 4. Results and Discussion

### 4.1. Suspension density of fluidizing magnetite particles

$\rho_{bM}$ of fluidizing magnetite particles is of great significance since it coarsely determines whether an introduced particle will float on the bed surface or deposit on the gas distributor. The variations of $\rho_{bM}$ with $U_g$ for the four types of magnetite particles are plotted in Fig. 4. As expected, $\rho_{bM}$ decreased monotonously with increasing $U_g$. The maximum $\rho_{bM}$ appearing at $U_g = U_{mfM}$ was always smaller than 2400 kg·m$^{-3}$, indicating that the gangue particles ($\rho_{pG} = 2613$ kg·m$^{-3}$) could always sink to the bottom simply as per the Archimedes principle. On the other hand, the characteristic $U_g$ (denoted as $U_{gc}$) corresponding to $\rho_{bM} = \rho_{pC} = 1459$ kg·m$^{-3}$ was also labeled in Fig. 4. It pointed out the maximum $U_g$ that could be exerted when the original intention was to separate the coal particles from the top surface of the ADMFB.

### 4.2. Lower size limit for gangue particles to sink

Recall the assumption from Section 2 that provided $\eta_{G,low}$ is greater than 50%, the gangue particles can potentially settle from the magnetite particles and be withdrawn from the bottom of the ADMFB. Nevertheless, as illustrated in Fig. 5, $\eta_{G,low}$ varied remarkably with $U_g$ for a given binary mixture of magnetite and gangue particles, indicating different potentials of separation. Then the key question arises: Which $\eta_{G,low}$ could best reflect the possibility of separation?

For each binary mixture, the deviation of $\eta_{G,low}$ away from 50% decreased rapidly with $U_g$ increasing from $U_{mfM}$ to high values. This phenomenon indicated that segregation between the magnetite and gangue particles diminished gradually as the gas flow increased, which agreed with the common sense [45]. Consequently, if the gangue particles could not accumulate in the lower half bed even at low gas velocities, the accumulation could no way occur at high gas velocities. To conclude, $\eta_{G,low}$ corresponding to $U_g = U_{mfM}$ reflected the maximum potential for the gangue particles to sink and be separated from the medium particles. Such a characteristic $\eta_{G,low}$ was denoted as $\eta_{Gm,low}$ which will be used hereafter for further analysis. Precisely, if $\eta_{Gm,low}$ was measured to exceed 50%, the gangue particles could deposit and be subsequently separated from the bottom of the ADMFB. On the other hand, the $\eta_{Gm,low}$ smaller than 50% indicated that the gangue particles could no way accumulate in the lower half bed, let alone to be extracted from the bottom. Based on this benchmark, $d_{pGc}$ corresponding to given magnetite particles could be determined simply from analyzing the change of $\eta_{Gm,low}$ with $d_{pG}$.

As for the four types of magnetite particles, the exact variations of $\eta_{Gm,low}$ with $d_{pG}$ are summarized and compared in Fig. 6. When the magnetite particles were given, $\eta_{Gm,low}$ was measured to drop

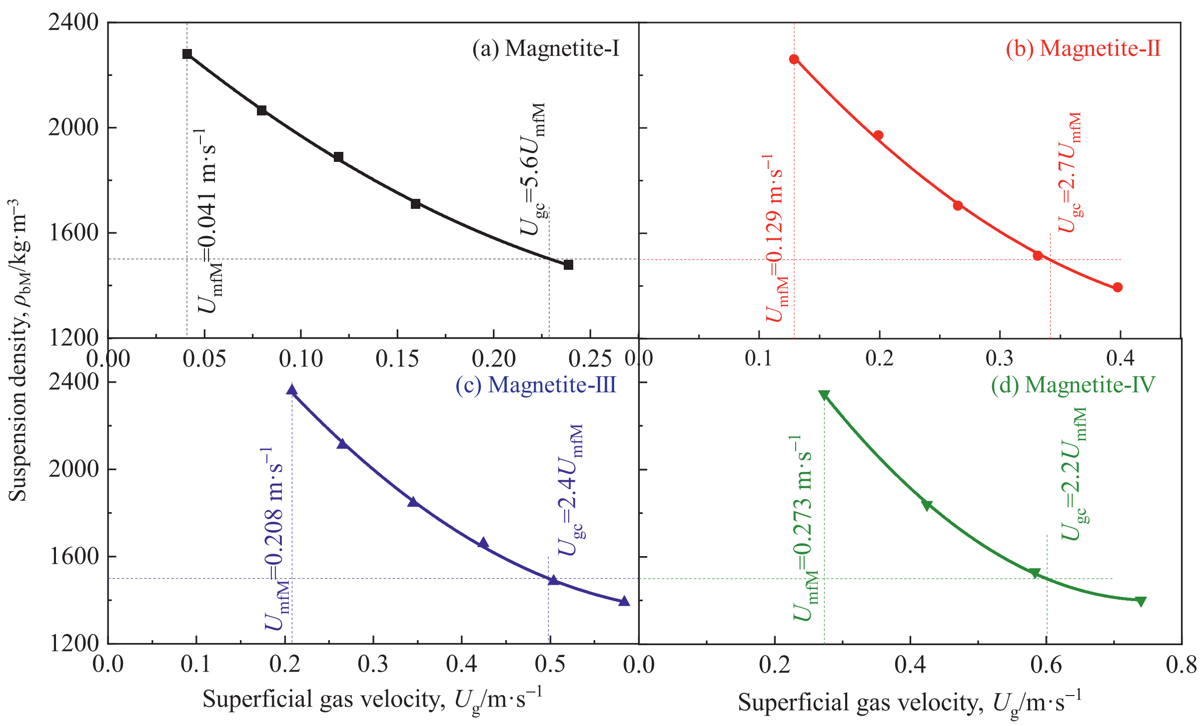


**Fig. 4.** Suspension density of fluidizing magnetite particles.

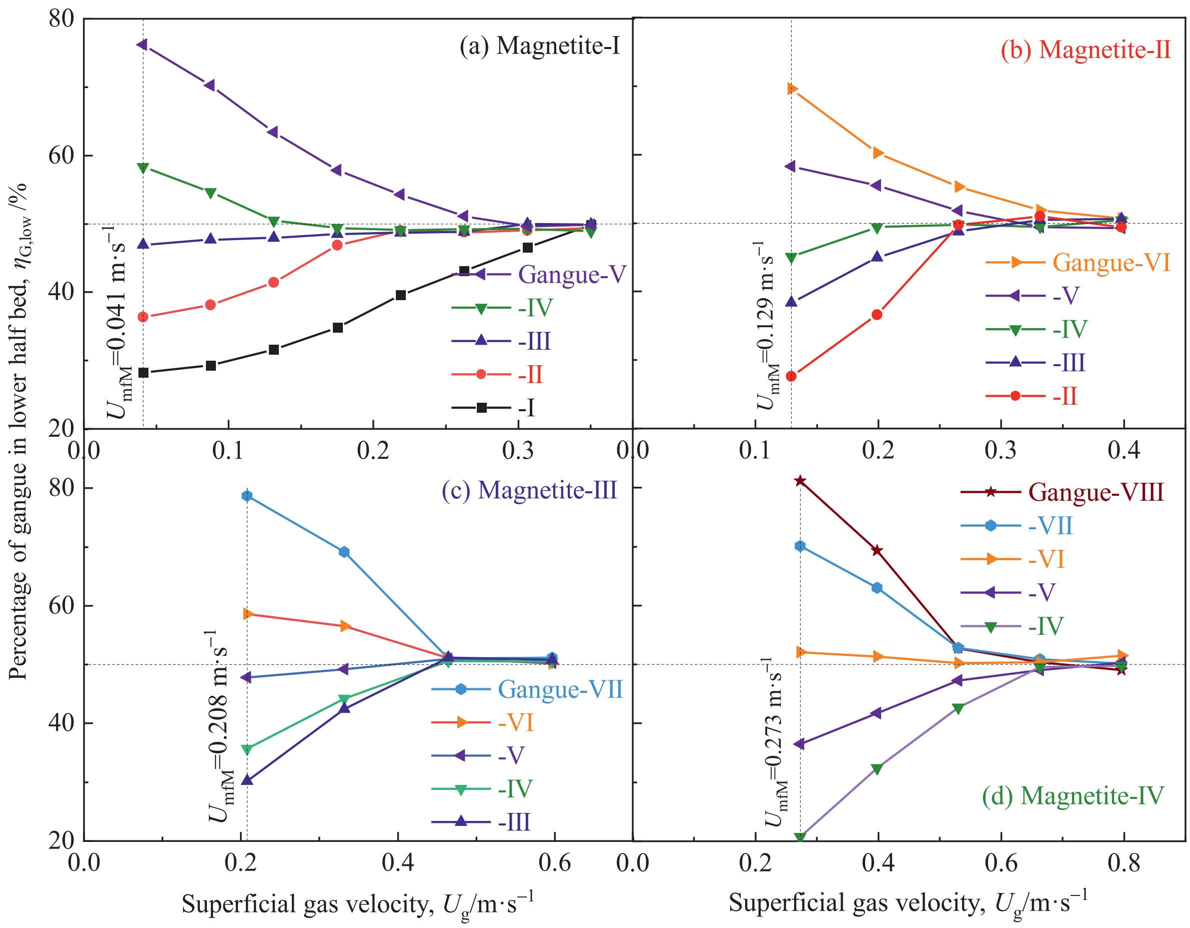


**Fig. 5.** Variations of $\eta_{G,low}$ with $U_g$ for binary mixtures of magnetite and gangue particles.

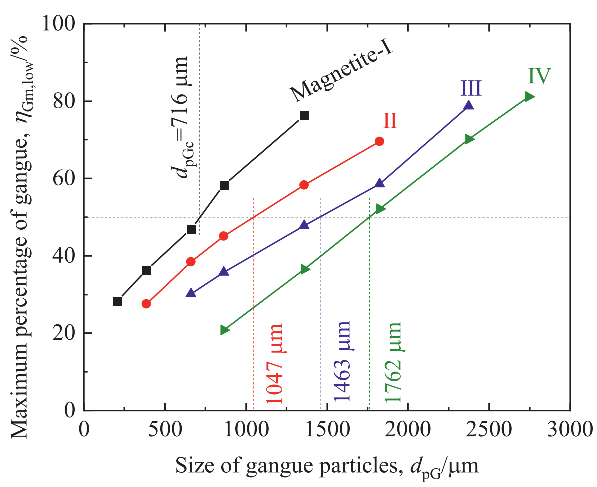


**Fig. 6.** Variations of $\eta_{Gm,low}$ with $d_{pG}$ for magnetite-I to -IV particles.

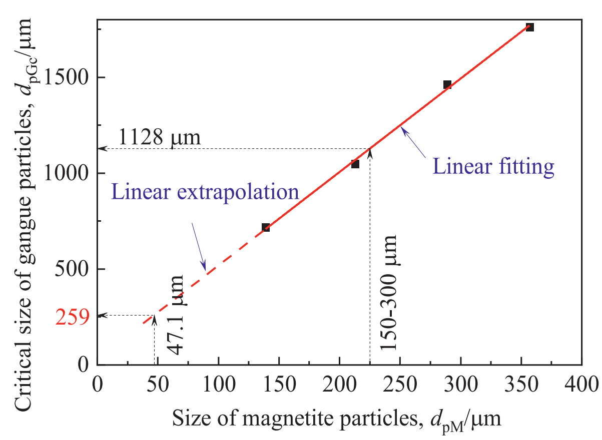


**Fig. 7.** Variations of $d_{pGc}$ with $d_{pM}$ for the gangue–magnetite binary mixture.

from >50% to <50% with decreasing $d_{pG}$. Precisely, $d_{pGc}$ could be defined as the $d_{pG}$ at which $\eta_{Gm,low}$ was equal to 50%. It can be clearly seen from Fig. 6 that $d_{pGc}$ differed for the four types of magnetite particles with distinct sizes. The exact variation of $d_{pGc}$ with decreasing $d_{pM}$ is further plotted in Fig. 7. The relationship could be linearly fitted by Eq. (1) where both terms are in micrometer.

$$d_{pGc} = 31.5 + 4.87 d_{pM} \tag{1}$$

The decrease trend of $d_{pGc}$ with decreasing $d_{pM}$ was of paramount significance. First and foremost, it demonstrated the feasibility of using fine magnetite particles to accommodate the small gangue particles. As for the 150–300 μm sized magnetite particles prevailed in the current ADMFB, $d_{pGc}$ could be identified as 1128 μm from Fig. 7. This phenomenon agreed well with the report that raw coal coarser than 6 mm could be handled effectively by the air-fluidized bed with such magnetite particles.

Furthermore, recall from Section 2 that $d_{\rm pMm}$ could be determined from the border between Geldart-B and -A groups. As illustrated in Fig. 1, such a critical size equaled 47.1 μm which was close to that (45 μm for magnetite particles with $\rho_{\rm pM} = 5200\ {\rm kg\cdot m^{-3}}$) reported in the Refs. [14,24]. Then, based on the linear extrapolation of Eq. (1), $d_{\rm pGc}$ corresponding to $d_{\rm pM} = 47.1$ μm could be derived as 259 μm. Only the gangue particles coarser than this critical size could be potentially separated from the bottom of the conventional ADMFB. If the gangue particles were finer than this critical size, they could not accumulate in the lower half of the ADMFB, much less to be withdrawn from the bottom.

Note additionally from Fig. 5 that for given magnetite particles fluidized at a given $U_{\rm g}$, $\eta_{\rm Gm,low}$ for the gangue particles with different sizes could vary in between <50% and >50%. This phenomenon confirmed the deduction in the Introduction that whether an introduced particle would sink or not in the fluidized bed depended not merely on its density but also on its size. The heavy gangue particles with a small size might not be able to sink owing to the turbulent gas–solid flow inside the bed. This behavior differed significantly from the sinking behavior of particles in a static liquid (depending merely on the density), eventually causing the difficulty in beneficiating the fine raw coal. In summary, the floating and sinking of fine particles depend not merely on the balance between the gravity and buoyancy. They are strongly affected by the drag force exerted by the rising of gas bubbles and the internal circulation of medium particles.

### 4.3. Lower size limit for coal particles to float

Recall from Section 2 that provided $\eta_{\rm C,up}$ is greater than 50%, there is potential to separate the coal particles from the top surface of the ADMFB with magnetite particles. Nevertheless, as illustrated in Fig. 8, $\eta_{\rm C,up}$ varied significantly with $U_{\rm g}$ for a given binary mixture of magnetite and coal particles, implying different potentials of separation. The $\eta_{\rm C,up}$ at which $U_{\rm g}$ could best reflect the potential of separation requires rigorous defense.

For each binary mixture, $\eta_{\rm C,up}$ was observed to approach downwards 50% with $U_{\rm g}$ increasing from $U_{\rm mfM}$ to $U_{\rm gc}$, implying that segregation between the magnetite and coal particles diminished gradually with increasing $U_{\rm g}$. In this case, if the coal particles can float from the magnetite particles even at $U_{\rm g} = U_{\rm gc}$, they could always float to the surface and further be extracted from the top surface. To conclude, $\eta_{\rm C,up}$ corresponding to $U_{\rm g} = U_{\rm gc}$ could reflect the minimum potential of segregation. It was specified as $\eta_{\rm Cm,up}$ which will be used hereafter for analyzing the possibility of separation. Precisely, if even $\eta_{\rm Cm,up}$ was measured to be greater than 50%, the coal particles could always precipitate from the magnetizable particles and be withdrawn from the top surface. Based on this benchmark, $d_{\rm pCc}$ corresponding to given magnetite particles could be determined from analyzing the variation of $\eta_{\rm Cm,up}$ with

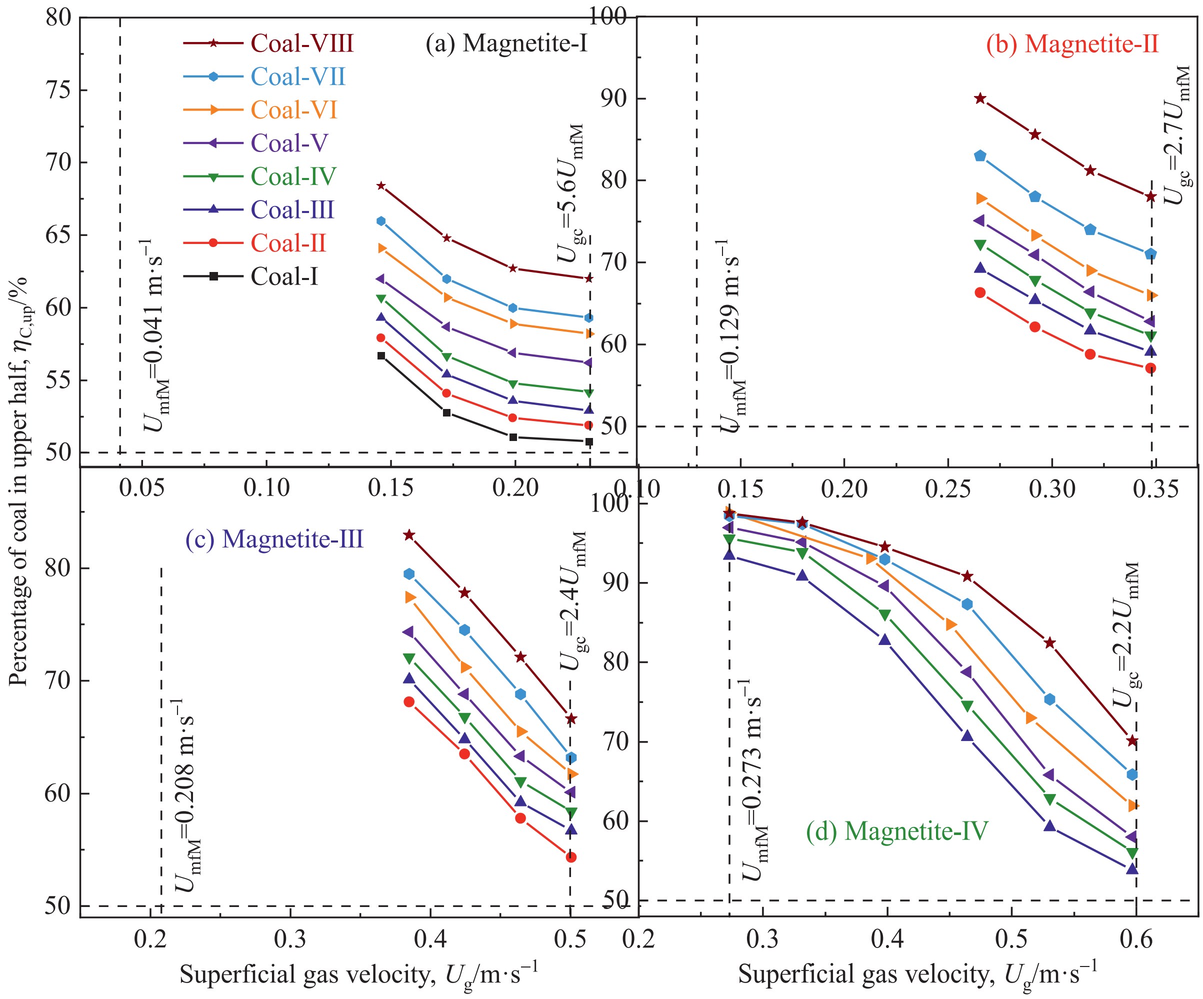


**Fig. 8.** Variations of $\eta_{\rm C,up}$ with $U_{\rm g}$ for binary mixtures of magnetite and coal particles.

$d_{pC}$. To be specific, $d_{pCc}$ could be identified as the $d_{pC}$ at which $\eta_{Cm,up}$ was equal to 50%.

As can be seen from Fig. 9, $\eta_{Cm,up}$ decreased monotonously with decreasing $d_{pC}$. Nevertheless, it never dropped below 50%. There seemed to be no concept of $d_{pCc}$ at all (much less $d_{pCm}$). The coal particles could always float in the conventional ADMFB with magnetite particles and subsequently be extracted from the top surface.

However, there was another problem related to the separation of fine coal particles as per the Archimedes principle. When their terminal velocity ($U_{tC}$) became smaller than the $U_{mfM}$ for the magnetite particles, the coal particles would be blown out of the ADMFB before the magnetite particles reached the minimum fluidization condition [46], much less to be beneficiated. Fig. 10 plots the variation of $U_{tC}$ with $d_{pC}$. Herein $U_{tC}$ was calculated as per Eqs. (2)–(4) [45,47]. For the four types of magnetite particles used in this study, both $d_{pM}$ and $U_{mfM}$ are listed in Table 1. $d_{pCc}$ corresponding to the magnetite particles with a given size of $d_{pM}$ could be identified by letting $U_{tC}$ equal $U_{mfM}$. The identification of $d_{pCc}$ for the magnetite-III particles ($d_{pM}$ = 289 μm, $U_{mfM} = 0.208\ \text{m}\cdot\text{s}^{-1}$) is exemplified in Fig. 10. The identified variation of $d_{pCc}$ with $d_{pM}$ is further plotted in Fig. 11 which was the $d_{pCc}$–$d_{pM}$ relationship mentioned in Section 2. Such a relationship could be well fitted by Eq. (5) where both terms are in micrometer. Based on such a relationship, $d_{pCc}$ corresponding to the 47.1 μm sized magnetite particles could be extrapolated as 9.8 μm. When $d_{pC}$ was smaller than 9.8 μm, $U_{tC}$ would become smaller than the $U_{mfM}$ corresponding to $d_{pMm}$ = 47.1 μm, indicating that coal particles finer than 9.8 μm could no longer be handled in the ADMFB with magnetite particles. Finally, $d_{pCm}$ could be identified as 9.8 μm.

$$u_{tC} = \left[\frac{4}{3}\frac{g d_{pC}(\rho_{pC}-\rho_g)}{C_D \rho_g}\right]^{0.5} \tag{2}$$

$$C_D = \begin{cases} 24/Re_{pC} & Re_{pC} < 0.4 \\ 10/Re_{pC}^{0.5} & 0.4 < Re_{pC} < 500 \\ 0.43 & 500 < Re_{pC} < 2\times10^5 \end{cases} \tag{3}$$

$$Re_{pC} = \frac{d_{pC} u_{tC} \rho_g}{\mu_g} \tag{4}$$

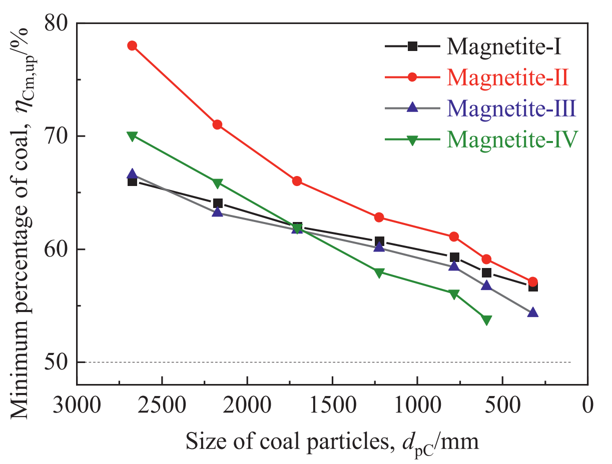


**Fig. 9.** Variations of $\eta_{Cm,up}$ with $d_{pC}$ for the four types of magnetite particles.

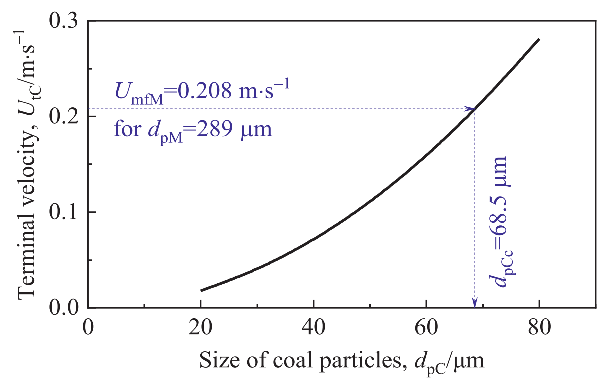


**Fig. 10.** An example of deriving $d_{pCc}$ from $d_{pM}$.

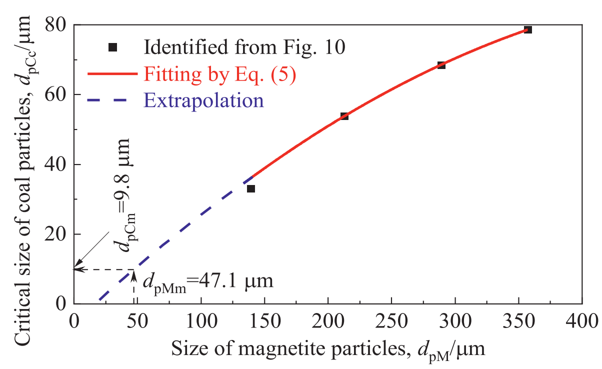


**Fig. 11.** Variations of $d_{pCc}$ with $d_{pM}$ for the coal–magnetite binary mixture.

$$d_{pCc} = -6.907 + 0.353 d_{pM} - 3.180\times10^{-4} d_{pM}^2 \tag{5}$$

### *4.4. Actual separation between gangue and coal particles*

Based on the findings achieved in Section 4.2, the lower size limit for the gangue component to sink was 259 μm. As per the findings in Section 4.3, the minimum size for the coal component to float was 9.8 μm. According to the compromise established in Section 2, the lower size limit of raw coal for the efficient dry beneficiation in the air-fluidized bed with magnetite particles can be determined as 259 μm. Finer raw coal will suffer severely from the remixing of separated gangue particles or the carryover of coal particles. It can be further concluded from the deviation of $d_{pGm}$ and $d_{pCm}$ that the difficulty in beneficiating the fine raw coal arises more from the remixing of sorted gangue particles than that of separated coal particles. This conclusion agreed well with the semi-industrial experimental data reported by Fu and coworkers [11].

Fig. 12 shows the actual separation performance between the gangue particles (275 μm) and coal particles (278 μm) in the air-fluidized bed with the 54.8 μm sized magnetite particles ($U_g = 2U_{mfM} = 0.01\ \text{m}\cdot\text{s}^{-1}$). The detailed size distributions of these three types of particles can be found in the Supplementary Material. Note particularly that as per normal operation [10], the gangue and coal particles were gradually poured into the bed after the fluidization of magnetite particles reached equilibrium. Both $\eta_{C,up}$ (52.2%) and $\eta_{G,low}$ (50.9%) were calculated to exceed the average (50%). This phenomenon confirmed the above conclusion that raw coal greater than 259 μm could be handled effectively in the air-

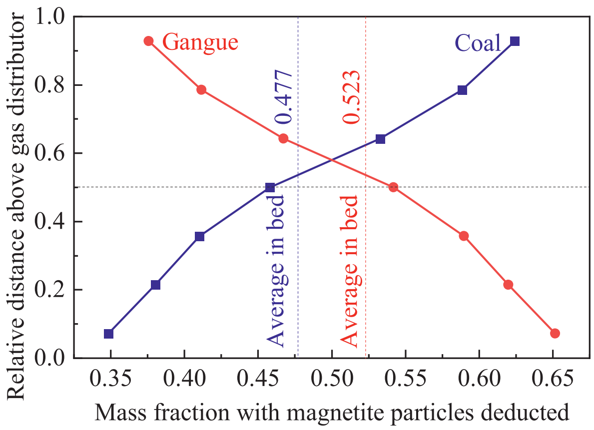


**Fig. 12.** Separation between 275 μm sized gangue particles and 278 μm sized coal particles in the ADMFB with 54.8 μm sized magnetite particles.

fluidized bed with the 47.1 μm sized magnetite particles. Moreover, the mass fraction of coal particles (for the coal–gangue binary mixture, the magnetite particles being deducted) increased monotonously as the distance above the gas distributor increased with the maximum reaching 0.624. In the top layer, such a fraction was raised by 31%. On the other hand, the mass fraction of gangue particles (for the coal–gangue binary mixture, the magnetite particles being deducted) increased as it became closer to the gas distributor with the maximum exceeding 0.652. In the bottom layer, such a fraction was raised by 24.7%. This phenomenon confirmed the conclusion drawn in the previous paragraph that the purification of the gangue component was more difficult than that of the coal component. Such a difficulty resulted probably from the stronger disturbance just above the gas distributor since the fluidizing air entered there.

The minimum magnetite particles that could be used in the ADMFB was reckoned to correspond to the border between Geldart-A and -B groups in this study. This was because the Geldart-A magnetite particles was reported to show a poor fluidization quality. This phenomenon resulted probably from that the magnetite particles had much stronger interparticle forces. The flow of magnetite particles were observed to be much more vicious than that of coal or gangue particles. An increase in the interparticle forces could make the Geldart-B particles turn into Geldart-A type [48]. In other words, whether the given particles belong to Geldart-A or -B type depended not only on their size but also on the interparticle forces. As far as we know, the magnetite particles ranging from 45 μm to 100 μm were reported to belong to Geldart-A type [32].

## 5. Conclusions

The lower size limit of raw coal for efficient beneficiation in the conventional ADMFB with magnetite particles was clarified in this work. Supposing the gangue particles accumulating in the lower half bed accounted for more than 50% of the feeding amount, they could be potentially withdrawn from the bottom. Assuming the coal particles residing in the upper half bed exceeded 50% of the feedstock, they could be extracted from the top surface. The feasibility of using small magnetite particles to accommodate the fine raw coal was confirmed from the experimental perspective. To realize smooth fluidization, $d_{pMm}$ was identified as 47.1 μm (the border between Geldart-B and -A groups), from which $d_{pGm}$ was derived as 259 μm whereas $d_{pCm}$ was deduced as 9.8 μm. Coal particles smaller than $d_{pCm}$ would be blown out of the ADMFB before the 47.1 μm sized magnetite particles became fluidized. The greater one between $d_{pGm}$ and $d_{pCm}$ eventually determined the $d_{pRm}$. The difficulty in beneficiating the fine raw coal was disclosed to result from the remixing of separated gangue particles rather than that of sorted coal particles. To promote the performance of beneficiating the fine raw coal in the ADMFB, more attention should be focused on the separation of gangue particles from the fluidizing magnetite particles.

## CRediT Authorship Contribution Statement

Yalong Cao: Investigation, Formal analysis. Donghui Liu: Writing – review & editing. Quanhong Zhu: Writing – review & editing, Writing – original draft, Supervision, Project administration, Funding acquisition, Conceptualization.

## Declaration of Competing Interest

The authors declare that they have no known competing financial interests or personal relationships that could have appeared to influence the work reported in this paper.


## Acknowledgements

This work was supported by Shandong Provincial Natural Science Foundation (ZR2023MB038) and Youth Innovation Team Program of Shandong Higher Education Institution (2022KJ156).


## Nomenclature

| | |
|---|---|
| $C_D$ | coefficient of drag, m |
| $d_p$ | average size of particles, m |
| $d_{pC}$ | average size of coal particles, m |
| $d_{pCc}$ | critical size of coal particles for given magnetite particles, m |
| $d_{pCm}$ | minimum size of coal particles, m |
| $d_{pG}$ | average size of gangue particles, m |
| $d_{pGc}$ | critical size of gangue particles for given magnetite particles, m |
| $d_{pGm}$ | minimum size of gangue particles, m |
| $d_{pM}$ | average size of magnetite particles, m |
| $d_{pMm}$ | minimum size of magnetite particles with smooth fluidization, m |
| $d_{pRm}$ | lower size limit of raw coal, m |
| $g$ | gravitational constant, $m \cdot s^{-2}$ |
| $L$ | inventory height, m |
| $Re_{pC}$ | particle Reynolds number at $U_g = U_{gc}$ |
| $U_g$ | superficial gas velocity, $m \cdot s^{-1}$ |
| $U_{gc}$ | critical $U_g$ at which $\rho_{bM} = 1500\ kg \cdot m^{-3}$, $m \cdot s^{-1}$ |
| $U_g/U_{mf}$ | fluidization number |
| $U_{mf}$ | minimum fluidization of particles, $m \cdot s^{-1}$ |
| $U_{mfC}$ | minimum fluidization of coal particles, $m \cdot s^{-1}$ |
| $U_{mfG}$ | minimum fluidization of gangue particles, $m \cdot s^{-1}$ |
| $U_{mfM}$ | minimum fluidization of magnetite particles, $m \cdot s^{-1}$ |
| $U_{tC}$ | terminal velocity of coal particles, $m \cdot s^{-1}$ |
| $\Delta P_b$ | bed pressure drop, kPa |
| $\Delta P_b$–$U_g\uparrow$ | bed pressure drop curve measured during increase of gas flow |
| $\rho_b$ | bulk density of particles, $kg \cdot m^{-3}$ |
| $\rho_{bM}$ | suspension density of magnetite particles, $kg \cdot m^{-3}$ |
| $\rho_g$ | density of air, $kg \cdot m^{-3}$ |
| $\rho_p$ | true density of particles, $kg \cdot m^{-3}$ |
| $\rho_{pC}$ | true density of coal particles, $kg \cdot m^{-3}$ |
| $\rho_{pG}$ | true density of guage particles, $kg \cdot m^{-3}$ |

$\rho_{pM}$ true density of magnetite particles, $kg \cdot m^{-3}$
$\eta_{C,up}$ percentage of feeding coal particles in upper half bed
$\eta_{Cm,up}$ critical $\eta_{C,low}$ at $U_g = U_{gc}$
$\eta_{G,low}$ percentage of feeding gangue particles in lower half bed
$\eta_{Gm,low}$ critical $\eta_{G,low}$ at $U_g = U_{mfM}$
$\mu_g$ viscosity of air, $Pa \cdot s$

## Supplementary Material

Supplementary data to this article can be found online at https://doi.org/10.1016/j.cjche.2025.05.009.

## References

[1] G.F. Li, D. Wang, Q.X. Liu, Y.M. Zhao, C.L. Duan, Separation performance of 0.5–1 mm fine coal in a gas–solid fluidized bed without dense medium, *Fuel* 318 (2022) 123645.
[2] Q.R. Chen, Y.F. Yang, Development of dry beneficiation of coal in China, *Coal Prep.* 23 (1–2) (2003) 3–12.
[3] G. Cheng, M.N. Zhang, Y. Lu, H.J. Zhang, E. Von Lau, New insights for improving low-rank coal flotation performance *via* emulsified waste fried oil collector, *Fuel* 357 (2024) 129925.
[4] R.A. Sahan, B. Kozanoglu, Use of an air fluidized bed separator in a dry coal cleaning process, *Energy Convers. Manag.* 38 (3) (1997) 269–286.
[5] R.A. Sahan, Coal cleaning performance in an air fluidized bed, *Energy Sources* 19 (5) (1997) 475–492.
[6] A.K. Sahu, S.K. Biswal, A. Parida, Development of air dense medium fluidized bed technology for dry beneficiation of coal—A review, *Int. J. Coal Prep. Util.* 29 (4) (2009) 216–241.
[7] L. Dong, Y.M. Zhao, C.L. Duan, Z.F. Luo, B. Zhang, X.L. Yang, Characteristics of bubble and fine coal separation using active pulsing air dense medium fluidized bed, *Powder Technol.* 257 (2014) 40–46.
[8] J. Choung, C. Mak, Z. Xu, Fine coal beneficiation using an air dense medium fluidized bed, *Coal Prep.* 26 (1) (2006) 1–15.
[9] P.F. Zhao, Y.M. Zhao, Z.Q. Chen, Z.F. Luo, Dry cleaning of fine lignite in a vibrated gas-fluidized bed: segregation characteristics, *Fuel* 142 (2015) 274–282.
[10] Y.M. Zhao, G.M. Li, Z.F. Luo, B. Zhang, L. Dong, C.C. Liang, C.L. Duan, Industrial application of a modularized dry-coal-beneficiation technique based on a novel air dense medium fluidized bed, *Int. J. Coal Prep. Util.* 37 (1) (2017) 44–57.
[11] Z.J. Fu, J. Zhu, S. Barghi, Y.M. Zhao, Z.F. Luo, C.L. Duan, Dry coal beneficiation by the semi-industrial air dense medium fluidized bed with binary mixtures of magnetite and fine coal particles, *Fuel* 243 (2019) 509–518.
[12] X.C. Fan, C.Y. Zhou, L. Dong, C.L. Duan, Y.M. Zhao, Coal beneficiation *via* the tapered fluidized bed using magnetite with a wide size range, *Mining Metall. Explor* 37 (3) (2020) 899–909.
[13] Y.M. Zhao, G.M. Li, Z.F. Luo, B. Zhang, L. Dong, Theory of modularized dry coal beneficiation and its application based on an air dense medium fluidized bed, *J. China Coal Soc.* 39 (8) (2014) 1566–1571. (in Chinese)
[14] S. Mohanta, C.S. Rao, A.B. Daram, S. Chakraborty, B.C. Meikap, Air dense medium fluidized bed for dry beneficiation of coal: technological challenges for future, *Part. Sci. Technol.* 31 (1) (2013) 16–27.
[15] S.L. Song, Y.M. Zhao, Z.F. Luo, L.G. Tang, X.L. Yang, Fine coal particles separation by air–solid magnetic stabilization, *J. China Coal Soc.* 37 (9) (2012) 1586–1590. (in Chinese)
[16] Z.G. Zhang, C. Xu, G. Cheng, E. Von Lau, Towards carbon neutrality: a comprehensive study on the utilization and resource recovery of coal-based solid wastes, *Int. J. Coal Sci. Technol.* 12 (1) (2025) 34.
[17] Z.F. Luo, Y.M. Zhao, Q.R. Chen, M.M. Fan, X.X. Tao, Separation characteristics for fine coal of the magnetically fluidized bed, *Fuel Process. Technol.* 79 (1) (2002) 63–69.
[18] Z.F. Luo, Y.M. Zhao, Q.R. Chen, X.X. Tao, M.M. Fan, Separation lower limit in a magnetically gas–solid two-phase fluidized bed, *Fuel Process. Technol.* 85 (2–3) (2004) 173–178.
[19] Z.F. Luo, Q.R. Chen, Effect of fine coal accumulation on dense phase fluidized bed performance, *Int. J. Miner. Process.* 63 (4) (2001) 217–224.
[20] Z.F. Luo, Q.R. Chen, Dry beneficiation technology of coal with an air dense-medium fluidized bed, *Int. J. Miner. Process.* 63 (3) (2001) 167–175.
[21] C.Y. Zhou, X.B. Liu, Y.M. Zhao, X.L. Yang, Y.J. Li, L. Dong, C.L. Duan, Z.H. Rao, Recent progress and potential challenges in coal upgrading *via* gravity dry separation technologies, *Fuel* 305 (2021) 121430.
[22] X.C. Fan, G.S. Zhang, Y.M. Zhao, C.Y. Zhou, L. Dong, C.L. Duan, Effect of middling coal on separation efficiency in air dense gas–solid fluidized bed, *Int. J. Coal Prep. Util.* 41 (9) (2021) 628–644.
[23] M.M. Fan, Q.R. Chen, Y.M. Zhao, Z.F. Luo, Fine coal (6–1 mm) separation in magnetically stabilized fluidized beds, *Int. J. Miner. Process.* 63 (4) (2001) 225–232.
[24] S. Mohanta, A.B. Daram, S. Chakraborty, B.C. Meikap, Characteristics of minimum fluidization velocity for magnetite powder used in an air dense medium fluidized bed for coal beneficiation, *Part. Part. Syst. Char.* 29 (4) (2012) 228–237.
[25] F.L. Guo, Gas flow and mixing behavior in fine-powder fluidized bed, *AIChE J.* 33 (11) (1987) 1895–1898.
[26] Y.M. Zhang, C.X. Lu, J.R. Grace, X.T. Bi, M.X. Shi, Gas back-mixing in a two-dimensional baffled turbulent fluidized bed, *Ind. Eng. Chem. Res.* 47 (21) (2008) 8484–8491.
[27] R.E. Rosensweig, W.K. Lee, J.H. Siegell, Magnetically stabilized fluidized beds for solids separation by density, *Separ. Sci. Technol.* 22 (1) (1987) 25–45.
[28] M.M. Fan, Q.R. Chen, Y.M. Zhao, Z.F. Luo, Study on fine coal separation in magnetically stabilized fluidized beds, *J. China Univ. Min. Technol.* 30 (6) (2001) 547–549. (in Chinese)
[29] M.M. Fan, Q.R. Chen, Y.M. Zhao, Z.F. Luo, Experimental research on dry coal separation by magnetically stabilized fluidized-bed, *Coal Prep. Tech* 30 (3) (2002) 6–8. (in Chinese)
[30] X.L. Yang, Y.M. Zhao, Z.F. Luo, S.L. Song, C.L. Duan, L. Dong, Fine coal dry cleaning using a vibrated gas-fluidized bed, *Fuel Process. Technol.* 106 (2013) 338–343.
[31] X.L. Yang, Y.M. Zhao, Z.F. Luo, Dry cleaning of fine coal based on gas–solid two-phase flow: a review, *Chem. Eng. Technol.* 40 (3) (2017) 439–449.
[32] C.G. Liu, C.Y. Zhou, Z.N. Sun, C.L. Duan, J. Zhu, Y.M. Zhao, Geldart $A^{-}$ particles: hydrodynamics of Geldart A magnetite powder with modulation by ultrafine coal particles in gas–solid fluidized bed coal beneficiator (GFBCB), *Powder Technol.* 408 (2022) 117753.
[33] D. Geldart, Types of gas fluidization, *Powder Technol.* 7 (5) (1973) 285–292.
[34] Q.H. Zhu, Q. Zhang, P.Y. Yang, H.J. Gai, M.Q. Lin, H.B. Song, M. Xiao, T.T. Huang, Measuring segregation in fluidized bed with magnetizable and non-magnetizable particles based on magnetic permeability, *Fuel* 340 (2023) 127554.
[35] R. Gujjula, N. Mangadoddy, Experimental investigation of hydrodynamics of gas–solid flow in an internally circulating fluidized bed, *Can. J. Chem. Eng.* 93 (8) (2015) 1380–1391.
[36] Q.H. Zhu, Y.L. Cao, Q. Zhang, W.K. Liu, H. Guan, D.H. Liu, H.J. Gai, Influences of polymorphism of packed particles on bulk characterizations in fluidization realm, *Chin. J. Chem. Eng.* 74 (2024) 238–248.
[37] Q.H. Zhu, Y.L. Cao, Q. Zhang, W.K. Liu, H. Guan, Universal methodology of measuring properties for particles based on their settled state in fluidized bed, *Fuel* 377 (2024) 132733.
[38] Q.H. Zhu, L.B. Zhang, W.K. Hao, Determining minimum fluidization velocity in magnetized fluidized bed with Geldart-B particles, *Powder Technol.* 389 (2021) 85–95.
[39] H.J. Gai, H.B. Song, M. Xiao, T.T. Huang, W.K. Hao, Q.H. Zhu, Improve reproducibility of determining minimum fluidization velocity *via* endowing it with a precise definition, *Part. Sci. Technol.* 41 (3) (2023) 341–349.
[40] Q. Liu, H.J. Gai, Q.H. Zhu, W.K. Hao, Effect of internal friction among unfluidized particles on measuring minimum fluidization velocity and segregation index, *Chem. Eng. Commun.* 210 (3) (2023) 348–360.
[41] Q.H. Zhu, Q. Zhang, P.Y. Yang, H.J. Gai, Z. Wang, H.B. Song, M. Xiao, T.T. Huang, Comparing two methods of acquiring stable fluidization state for binary particles during measurement of segregation, *Fuel* 346 (2023) 128410.
[42] B. Anicic, B.N. Lu, W.G. Lin, H. Wu, K. Dam-Johansen, W. Wang, CFD simulation of mixing and segregation of binary solid mixtures in a dense fluidized bed, *Can. J. Chem. Eng.* 98 (1) (2020) 412–420.
[43] S.M. Wu, B. Straiton, Y. Zong, Q. Marashdeh, L.Q. Li, Z.M. Xu, L. Zhao, A new measurement method for mixing and segregation of binary mixture by combining gas cutting-off method and ECVT, *Powder Technol.* 409 (2022) 117806.
[44] J.K. Huang, Y.J. Lu, H. Wang, A new quantitative measurement method for mixing and segregation of binary-mixture fluidized bed by capacitance probe, *Chem. Eng. J.* 326 (2017) 99–108.
[45] M. Kwauk, H.Z. Li, Handbook of Fluidization, Chemical Industry Press, Beijing, 2007. (in Chinese)
[46] N.C. Lockhart, Dry beneficiation of coal, *Powder Technol.* 40 (1–3) (1984) 17–42.
[47] D. Kunii, O. Levenspiel, Fluidization Engineering, second ed., Butterworth-Heinemann, Boston, 1991.
[48] M.J. Rhodes, X.S. Wang, A.J. Forsyth, K.S. Gan, S. Phadtajaphan, Use of a magnetic fluidized bed in studying Geldart group B to A transition, *Chem. Eng. Sci.* 56 (18) (2001) 5429–5436.